Bioorganic & Medicinal Chemistry 16 (2008) 8082–8089

Contents lists available at ScienceDirect

Bioorganic & Medicinal Chemistry

journal homepage: www.elsevier.com/locate/bmc

Spin trapping experiments with different carbamoyl-substituted EMPO derivatives

Klaus Stolze [a,*], Natascha Rohr-Udilova [b], Andreas Hofinger [c], Thomas Rosenau [c]

[a] Molecular Pharmacology and Toxicology Unit, Department of Biomedical Sciences, University of Veterinary Medicine Vienna, Veterinärplatz 1, A-1210 Vienna, Austria
[b] Division of Gastroenterology and Hepatology, Department of Internal Medicine III, Medical University of Vienna, Währinger Gürtel 18-20, A-1090 Vienna, Austria
[c] Department of Chemistry, University of Natural Resources and Applied Life Sciences (BOKU), Muthgasse 18, A-1190 Vienna, Austria

ARTICLE INFO

Article history:
Received 18 February 2008
Revised 17 July 2008
Accepted 22 July 2008
Available online 25 July 2008

Keywords:
EPR
Spin trapping
Superoxide
EMPO/AMPO derivatives

ABSTRACT

The spin trapping behavior of five carbamoyl-substituted EMPO derivatives, 5-aminocarbonyl-5-methyl-pyrroline *N*-oxide (CAMPO (AMPO)), 5-aminocarbonyl-5-ethyl-pyrroline *N*-oxide (CAEPO), 5-aminocarbonyl-5-propyl-pyrroline *N*-oxide (CAPPO), 5-aminocarbonyl-5-*n*-butyl-pyrroline *N*-oxide (CABPO), and 5-aminocarbonyl-5-*n*-pentyl-pyrroline *N*-oxide (CAPtPO), toward different oxygen- and carbon-centered radicals is described, the stabilities of the superoxide adducts ranging from about 8 to 17 min.

1. Introduction

Derivatives of the spin trap EMPO have previously been shown to possess increased superoxide adduct stabilities if an ethyl or methyl substituent is present in position 3 or 4 of the pyrroline ring.[1–3] The diastereomers in these compounds exhibited—due to the presence of two asymmetric carbon centers—significantly different spin trapping properties and spin adduct stabilities (e.g., *cis*- and *trans*-3,5-EDPO/·OOH: $t_{1/2}$ = 11 and 45 min, respectively). Recent publications by other groups suggested that these differences can also be used to distinguish between the formation pathways of spin adducts, for example, whether the hydroxyl radical adduct has been formed by the trapping of hydroxyl radicals or by reduction of initially formed superoxide adducts.[4]

Furthermore, it has been suggested that a better spin trapping performance can also be achieved if the ethoxycarbonyl group of EMPO is replaced by an aminocarbonyl group.[5,6] We therefore investigated the effect of different 5-alkyl substituents on the spin trapping performance of several 5-carbamoyl-substituted EMPO derivatives.

2. Results

2.1. Structure of the spin traps

All spin traps synthesized and investigated within this study can be considered as derivatives of the series 5-ethoxycarbonyl-5-methyl-1-pyrroline-*N*-oxide (EMPO), 5-ethoxycarbonyl-5-ethyl-1-pyrroline-*N*-oxide (EEPO), 5-ethoxycarbonyl-5-propyl-1-pyrroline-*N*-oxide (EPPO), 5-ethoxycarbonyl-5-*n*-butyl-1-pyrroline-*N*-oxide (EBPO), and 5-ethoxycarbonyl-5-*n*-pentyl-1-pyrroline-*N*-oxide (EPtPO), in which the ethoxycarbonyl substituent has been replaced by a $CONH_2$ group. Although the compound 5-carbamoyl-5-methyl-1-pyrroline-*N*-oxide has recently been referred to as 'AMPO[5]' we would like to use the abbreviations CAMPO, CAEPO, CAPPO, CABPO, and CAPtPO, respectively, for these compounds (CA = 5-carbamoyl–) in order to avoid confusion with the respective 5-alkoxycarbonyl-5-methyl-1-pyrroline *N*-oxides, also referred to as 'AMPO[7]' (for structures, see Fig. 1A). A general synthetic scheme is given in Figure 1B.

Structural identity of the novel spin traps was confirmed by ^{13}C NMR (Table 1), ^{1}H NMR (Table 2), ESI Q-TOF MS analysis (Table 3), FTIR spectroscopy (Table 4), and UV–vis spectroscopy (Table 5).

A complete set of ^{1}H, H–H correlated, ^{13}C, HMQC, and HMBC spectra was recorded for each compound, which allowed for a complete signal assignment in both the ^{1}H and ^{13}C domains. Carbon NMR confirmed the presence of a heterocyclic pyrroline ring. The resonances for C-2 were found around 135.4–138.2 ppm, mostly down-field shifted by about 1.1 ppm compared to the respective esters (134.9–136.3 ppm), those for C-3 (22.5–28.2 ppm) varied considerably more compared to the esters (25.4–26.3 ppm), a significant up-field shift being detectable for CABPO (−3.5 ppm) and CAPtPO (−3 ppm), those for C-4 (25.1–30.6 ppm) were up-field shifted by about 2 ppm compared to the esters (27.4–31.9 ppm), and those for C-5 ranged between 79.2 and 81.9 ppm, comparable to the esters (78.5–82.1 ppm).

* Corresponding author. Tel.: +43 1 25077 4406; fax: +43 1 25077 4490.
E-mail address: Klaus.Stolze@vu-wien.ac.at (K. Stolze).

0968-0896/$ - see front matter © 2008 Elsevier Ltd. All rights reserved.
doi:10.1016/j.bmc.2008.07.057

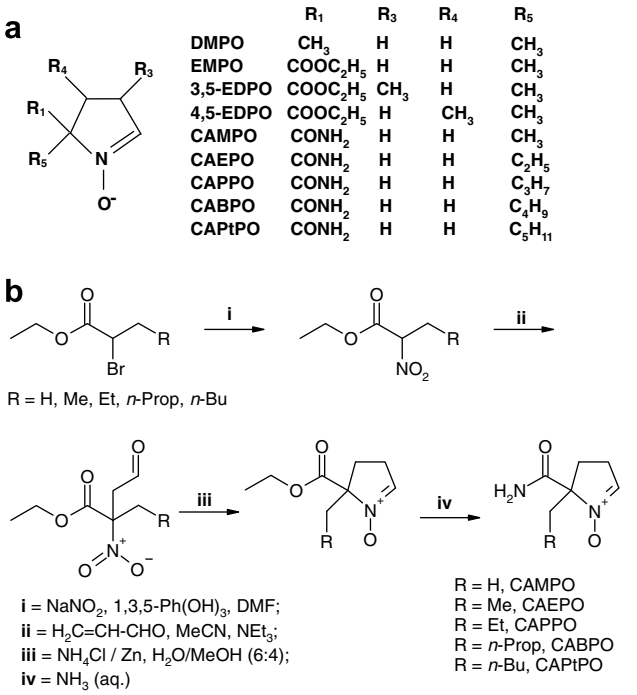

Figure 1. (a) General structure of the spin traps and (b) general synthetic scheme.

The shift of the aminocarbonyl group was down-field shifted by about 2.5 ppm to values between 170.5 and 174.7 ppm compared to the ethoxycarbonyl group of the esters (169.3–170.3 ppm).

In contrast to this structure, the resonances of the $^{1''}C$ of the 5-alkyl substituents were much more dependent on the substituent. The proton spectra also showed typical resonance patterns. H-2 exhibited coupling constants of around 2.5 Hz and appeared as a triplet. The triplet pattern of H-2—not a doublet of doublets—indicated similar coupling constants to the geminal H-3 protons. Due to the diastereotopic properties of the amide group (restricted rotation around the C-N bond as a consequence of its partial double bond character due to π-conjugation), the NH_2 protons appeared as two separate resonances, their difference steadily increasing from CAMPO (AMPO) (7.16 and 7.38 ppm) to CAPtPO (5.81 and 8.40 ppm). It should be noted that such comparisons are only possible if the spectra were recorded under strictly similar conditions with regard to concentration, temperature, and solvent. The resonances of the 5-alkyl substituents were comparable in the carbamoyl and the ester derivatives.

The diastereotopic protons of the methylene groups in the pyrroline ring at C-3 and C-4 of the carbamoyl compounds appeared in the same range as in the respective esters, but their diastereotopic splitting was, however, somewhat more pronounced.

The major absorption peaks in the respective FTIR spectra were around 1680 cm^{-1} (C=O), 1580 cm^{-1} (C=N), and 1205 cm^{-1} (N–O). The absorbances around 3150 cm^{-1} and 3350 cm^{-1} (N–H valence bands) are not always well resolved and, in addition, very

Table 1
^{13}C NMR data (ppm) of the spin traps

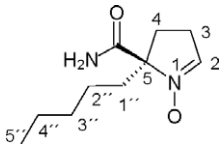

	^{2}C	^{3}C	^{4}C	^{5}C	CO	$^{1''}C$	$^{2''}C$	$^{3''}C$	$^{4''}C$	$^{5''}C$
EMPO[12]	134.9	25.4	31.9	78.5	169.3	20.3	–	–	–	–
CAMPO (Lit.)[5]	135.6	25.3	30.6	79.2	174.7	22.5	–	–	–	–
	137.4	25.0	30.5	79.1	172.9	24.2	–	–	–	–
CAEPO	136.6	28.2	26.1	81.5	171.5	24.6	7.5	–	–	–
CAPPO	138.2	24.7	26.9	81.9	172.4	38.5	16.8	14.0	–	–
CABPO	137.2	22.5	25.4	81.8	172.3	36.2	26.9[a]	24.9[a]	13.7	–
CAPtPO	135.4	23.2	25.1	80.2	170.5	34.8	21.3[b]	29.8	20.6[b]	12.2

[a,b] Tentative assignment (reversed order also possible).

Table 2
^{1}H NMR data (ppm) of the spin traps

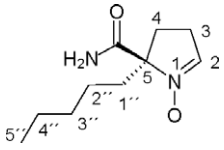

	^{2}CH	$^{3}CH_2$	$^{4}CH_A$	$^{4}CH_B$	NH_A	NH_B	$^{1''}CH_x$	$^{2''}CH_x$	$^{3''}CH_x$	$^{4''}CH_x$	$^{5''}CH_3$
EMPO[12]	6.97t	2.75m	2.16m	2.60m	4.26m[a]	1.31t[b]	1.72s	–	–	–	–
CAMPO (Lit.)[5]	6.97t	2.46–2.53m	1.96–2.03m	2.58–2.62m	7.16s	7.38s	1.73s	–	–	–	–
	7.19t	2.79m	2.27–2.34m	3.14–3.20m	5.85b	8.46b	1.90s	–	–	–	–
CAEPO	7.09t	2.44–2.49m	2.04–2.09m	2.49–2.58m	7.38b	7.85b	1.83–1.92m	0.81t	–	–	–
CAPPO	6.99t	2.49–2.58m	2.08–2.15m	2.82–2.89m	6.16b	8.26b	1.88–2.05m	1.18–1.40m	0.90t	–	–
CABPO	7.03t	2.55–2.66m	2.13–2.23m	2.90–3.00m	5.95b	8.41b	1.99–2.12m	1.26–1.37m	1.26–1.37m	0.89t	–
CAPtPO	7.02t	2.51–2.68m	2.14–2.22m	2.91–2.99m	5.81b	8.40b	1.96–2.12m	1.28–1.36m	1.28–1.36m	1.28–1.36m	0.89t

Abbreviations: s, singlet; b, broad singlet; t, triplet; m, multiplet.
[a] From ethoxy group $^{1'}CH_2$.
[b] From ethoxy group $^{2'}CH_3$.

Table 3
ESI Q-TOF HR-MS analysis of the spin traps

Sample	Acquired $[MH]^+$	Calcd $[MH]^+$	Error (ppm)	mDa	Acquired $[MNa]^+$	Calcd $[MNa]^+$	Error (ppm)	mDa
CAMPO	143.08543	143.0820	23.97	3.43	165.06934	165.0640	32.35	5.34
CAEPO	157.10249	157.0976	31.13	4.89	179.0852	179.0796	31.27	5.60
CAPPO	171.11634	171.1132	18.35	3.14	193.09918	193.0952	20.61	3.98
CABPO	185.13436	185.1288	30.03	5.56	207.11692	207.1108	29.55	6.12
CAPtPO	199.14548	199.1444	5.42	1.08	221.12958	221.1264	14.38	3.18

sensitive to traces of humidity. They are, therefore, not listed in Table 4.

2.2. Superoxide radical adducts

When CAEPO (20 mM) was incubated in the presence of 0.2 mM hypoxanthine/500 mU/ml xanthine oxidase in 20 mM oxygenated phosphate buffer (pH 7.4, 0.4 mM DTPA), an ESR spectrum consisting of a mixture of at least two different species was observed from the beginning, whose intensity increased steadily for about 10 min. At this point, 250 U/ml SOD was added and the spectrum recorded immediately thereafter (Fig. 2a). In order to obtain the spectra of individual components, the spectrum was recorded again after 30 min (Fig. 2b), resulting in a slightly different ratio of the components. The difference spectrum shown in Figure 2c (spectrum "a" subtracted from spectrum "b") represents the CAEPO superoxide adduct, which (assuming a mixture of two different isomers without taking into account a possible dynamic exchange[4]) can best be simulated using the following set of parameters (Fig. 2d): a_N = 13.18 G, a_H = 9.95 G, 53%, and a_N = 13.18 G, a_H = 12.25 G, 47%; ΔH = 1.75 G, ratio Gauss/Lorentz 1:1).

A typical exponential decay curve (CAEPO/·OOH, $t_{1/2}$ = 16.95 min, R^2 = 0.998) together with the respective exponential fit can be seen in Figure 3, obtained from intensity measurements of the low-field peak every 1.5 min, and after subtraction of the respective contribution of the secondary product mentioned below.

From the other spin traps investigated similar results were obtained (HFS parameters, see Table 6), except that secondary products were formed much faster, see Figure 4a for the secondary product formed from CAMPO (AMPO) and Figure 4b for its computer simulation (a_N = 14.43 G, a_H = 19.34 G, and a_N = 2.17 G, ΔH = 1.50 G, ratio Gauss/Lorentz 1:2). The formation of the secondary amino adduct was superoxide-dependent (no adduct formed when SOD was added prior to xanthine oxidase), and an identical secondary species was also detected in a system containing azide, hydrogen peroxide, and HRP. The expected azide radical adduct was barely visible and decayed rapidly (experiment not shown), whereas the relative intensity of the secondary amino adduct increased with time. Since these secondary products were formed under oxidizing conditions, we assume that the second amino group is located in position 5, formed according to a Hofmann degradation reaction.

An additional control experiment, where CAMPO (500 mM) was incubated with a sodium hypochlorite solution (2.5%) for 2 min, followed by 1:12 dilution with 150 mM phosphate buffer (pH

Table 5
Half-life of the superoxide adducts, *n*-octanol/buffer partition coefficients, and UV–vis spectroscopic data of the spin traps

Compound	Apparent $t_{1/2}$ (min) Xa/XOD	Partition coefficient *n*-octanol/phosphate buffer (100 mM, pH 7.0)	UV data λ_{max} and molar absorptivity ε
EMPO[12]	8.6[12]	0.15[12]	231 nm, 7417 ± 46
CAMPO	8.58 ± 0.86	0.016 ± 0.002	232 nm, 7652 ± 43
CAEPO	16.76 ± 0.36	0.056 ± 0.001	233 nm, 7906 ± 28
CAPPO	10.40 ± 0.25	0.211 ± 0.003	233 nm, 7508 ± 14
CABPO	10.65 ± 0.25	0.668 ± 0.004	233 nm, 7741 ± 55
CAPtPO	11.13 ± 0.21	2.72 ± 0.05	234 nm, 6885 ± 39

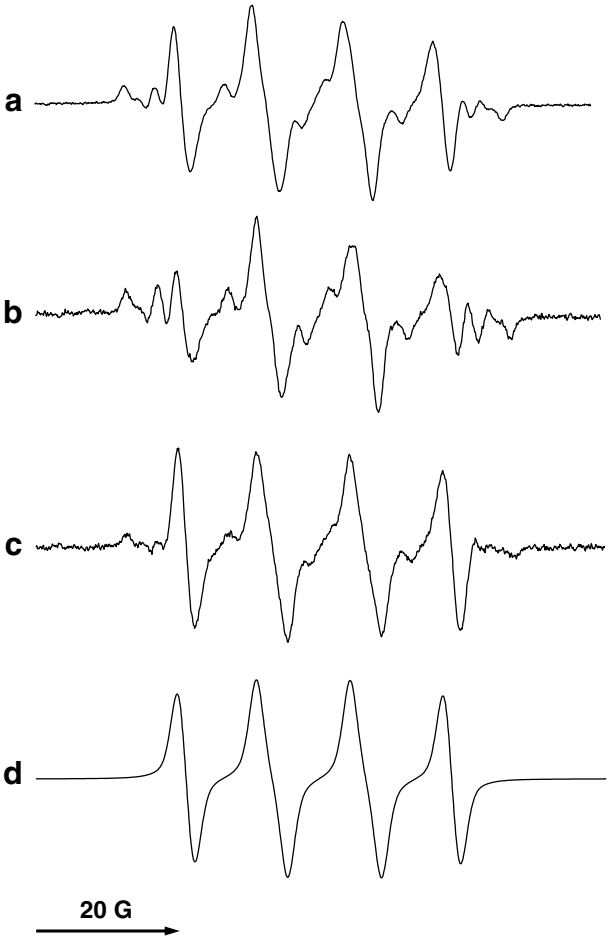

Figure 2. Mixture of radicals formed from the spin trap CAEPO incubated with hypoxanthine/xanthine oxidase. (a) CAEPO (20 mM), catalase (250 U/mL), hypoxanthine (0.2 mM), and xanthine oxidase (500 mU/mL) in oxygenated phosphate buffer (20 mM, pH 7.4, containing 0.4 mM DTPA) were incubated for 10 min, the reaction stopped upon addition of SOD (250 U/ml) and measured using the following EPR parameters: sweep width, 80 G; modulation amplitude, 0.5 G; microwave power, 20 mW; time constant, 0.08 s; receiver gain, 1×10^5; scan rate, 57 G/min. (b) Spectrum recorded for 30 min after (a), (c) difference (a − b), showing the CAEPO superoxide adduct (d); and simulation of the spectrum.

Table 4
IR data (cm^{-1}) of the spin traps

EMPO[12]	*2985*	*2940*	2874	**1741**	–	**1582**	*1464*	*1446*	*1377*	1341	*1288*	**1236**	**1182**	**1107**	–	*1024*	–	950	926	*862*	796	–	–	–
CAMPO	*3047*	2939	2784	**1679**	1630	*1587*	1475	*1446*	*1396*	1379	*1298*	*1218*	*1199*	1115	1097	1029	998	953	885	843	744	700	*656*	*611*
CAEPO	2974	2940	2883	**1680**	–	*1580*	*1463*	–	*1386*	–	1288	**1208**	*1157*	1124	1037	–	985	940	–	–	798	–	*694*	*623*
CAPPO	**2963**	**2930**	*2875*	**1680**	**1614**	**1579**	*1464*	–	*1383*	*1350*	1293	**1205**	*1181*	*1122*	1042	1020	981	941	–	–	*796*	–	*693*	**624**
CABPO	**2957**	**2930**	**2870**	**1681**	**1614**	**1577**	*1462*	–	*1381*	–	1294	**1202**	–	1124	–	1024	–	949	–	–	792	*696*	*624*	*603*
CAPtPO	*2956*	*2927*	*2862*	**1682**	*1613*	*1555*	1460	–	1381	–	1286	1221	*1200*	1123	–	1011	–	954	–	–	796	696	628	602

Intensities: strong (**1741**), medium (*1464*), weak (950).

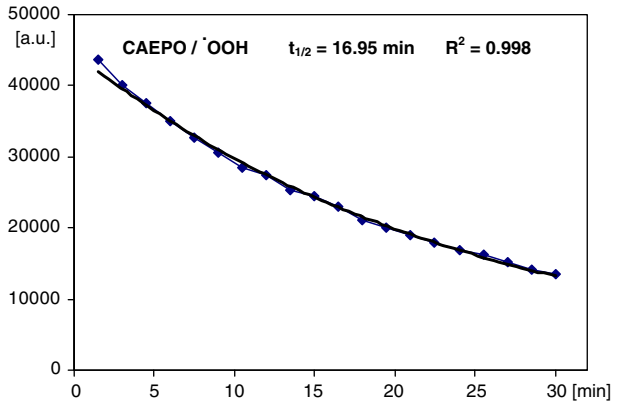

Figure 3. Decay kinetics of the CAEPO/˙OOH radical adduct ESR spectra of the CAEPO/˙OOH adduct (see above, Fig. 2a) were recorded at 1.5 min intervals for 30 min, the secondary product formed subtracted from each individual spectrum and the intensity of the low-field peak measured (in arbitrary units). From the exponential fit shown above (apparent first order) $t_{1/2}$ = 16.95 min and r^2 = of 0.998 were calculated.

7.4, containing 10 mM DTPA), also resulted in the formation of the same secondary species (not shown). From these observations it can be concluded that the second nitrogen splitting from this secondary product stems from an amino group attached to position 5 (formed upon oxidative degradation of the carbamoyl group to an amino group). The structure is in agreement with the HFS parameters of the DMPO amino adduct previously reported by Chignell et al.[8] (a_N = 15.9 G, a_H = 19.3 G, a_N = 1.6 G) and by Kirino et al.[9] (a_N = 15.86 G, a_H = 19.04 G, a_N = 1.72 G). Without isotope labeling (using 50% $^{15}N/^{15}N$ plus 50% $^{14}N/^{14}N$ and looking for the formation of $^{14}N/^{15}N$ products) we cannot, however, rule out an intermolecular reaction pathway, leading to 2-amino substituted products.

From the other spin traps, less intensive ESR spectra were obtained from the respective secondary products, some of which were formed as mixtures of two stereoisomers, for example, from CABPO (Fig. 4c; a_N = 14.30 G, a_H = 19.75 G, a_N = 2.40 G, 53%; and a_N = 14.05 G, a_H = 16.30 G, a_N = 2.70 G, 47%), obtained by computer simulation (Fig. 4d). All data are summarized in Table 6.

Half-lives of the superoxide adducts were determined from a series of repetitive scans (every 90 s for 30 min) using a first-order exponential decay approximation (Table 5, Pearson correlation coefficient $R^2 > 0.97$). In all cases, secondary products were subtracted from each individual spectrum before the decay kinetics was calculated. In addition to a small contribution of the respective hydroxyl radical adducts probably formed due to partial hydrolysis of the spin adducts, increasing amounts of amino adducts were observed, especially with CAMPO (AMPO), where the observation of a neat superoxide adduct was virtually impossible.

2.3. Hydroxyl radical adducts

Incubation of CAMPO (AMPO) in the presence of a Fenton system resulted in the detection of the respective hydroxyl radical adduct (Fig. 5a). The spectrum consists of two different stereoisomers in the ratio 81/19, and was identified according to data recently presented by Villamena et al.[5] Similar results were obtained from CAEPO (Fig. 5b), CAPPO (Fig. 5c), CABPO (Fig. 5d), and CAPtPO (Fig. 5e). Except for the latter two, the spectra of the hydroxyl adducts remained detectable for more than 30 min.

2.4. Alkoxyl adducts from methanol and ethanol

Methanol and ethanol were chosen as model compounds for metabolites, for example, obtained from lipids after oxidation reactions. In principle, two different types of radical adducts can be formed from alcohols: oxygen-centered alkoxyl radical adducts and carbon-centered radical adducts. Alkoxyl radical adducts were synthesized by nucleophilic addition of methanol or ethanol, using a model system previously described by Dikalov et al.[10] and already tested with other spin traps.[1–3,11,12] As shown in Figure 6a, CAPPO/˙OCH_3 was obtained from methanol and iron-(III) chloride, the mixture of which was diluted 1:50 after 2 min with 300 mM phosphate buffer containing 20 mM DTPA. In the same manner, CAPPO/˙OC_2H_5 was obtained from ethanol and iron (III) chloride (Fig. 6b), CAPtPO/˙OCH_3 from methanol and iron-(III) chloride (Fig. 6c), and CAPtPO/˙OC_2H_5 from ethanol and iron-(III) chloride (Fig. 6d). All alkoxyl radical adducts remained only detectable for a short period of time (1–5 min), after which the more stable carbon-centered adducts became predominant.

2.5. Carbon-centered radical adducts from methanol and ethanol

In order to detect radical adducts of alcohol-derived carbon-centered radicals (i.e., the hydroxymethyl and the α-hydroxyethyl radicals), a Fenton-type system[13] was chosen consisting of the spin trap (40 mM), hydrogen peroxide (0.2%), EDTA (2 mM), and iron-(II) sulfate (1 mM) in a mixture of methanol (or ethanol, respectively) with water (20/80, v/v). After 10 s, the reaction was stopped upon 1:1 dilution with phosphate buffer (300 mM, pH 7.4) containing DTPA (20 mM). In Figure 7a, the hydroxymethyl radical adduct of CAPPO is shown, consisting of two different species (a_N = 14.53 G; a_H = 23.08 G; 63%, and a_N = 14.70 G; a_H = 20.82 G; a_H = 1.20 G; 37%), which can clearly be distinguished from the respective methoxyl radical adduct (a_N = 13.50 G; a_H = 9.69 G; 100%). In the same way, the adducts CAPPO/˙$CH(CH_3)OH$ (Fig. 7b), CAPtPO/˙CH_2OH (Fig. 7c), and CAPtPO/˙$CH(CH_3)OH$ (Fig. 7d) were obtained.

2.6. Carbon-centered radical adducts from formate

In order to detect the respective radical adducts of the carbon dioxide anion radical, a Fenton-type system[13] was chosen consisting of the spin trap CAMPO (40 mM), hydrogen peroxide (0.2%), EDTA (2 mM), and iron-(II) sulfate (1 mM) in aqueous sodium formate solution (200 mM). After 10 s, the reaction was stopped upon 1:1 dilution with phosphate buffer (300 mM, pH 7.4) containing DTPA (20 mM) (a_N = 14.46 G; a_H = 16.62 G; 58%; and a_N = 14.20 G; a_H = 18.30 G; 42%; Fig. 8a). Similarly, the adducts CAEPO/·CO_2^- (Fig. 8b; a_N = 14.04 G; a_H = 19.31 G; 100%), CAPPO/·CO_2^- (Fig. 8c), CABPO/·CO_2^- (Fig. 8d), and CAPtPO/·CO_2^- (Fig. 8e) were obtained.

In the same way, the respective methyl adducts were formed, except that DMSO (10%) was used instead of formate (spectrum not shown). For detection of the H adducts, the respective spin traps were incubated in the presence of a small amount of KBH_4 (ca. 0.5 mg/500 μl) for 1 min, after which the pH was readjusted to pH 7.4 by dilution with phosphate buffer (300 mM, pH 7.4).

An overview of the spin adducts of all investigated spin traps and the comparison with the respective EMPO adducts is given in Table 6.

3. Discussion

Four novel amino derivatives of the spin trap EMPO were synthesized in this study and compared with a fifth, CAMPO (AMPO), the synthesis and properties of which have recently been described elsewhere.[5,6] The structure of the compounds was comprehensively characterized by full NMR assignment (^1H and ^{13}C), ESI Q-TOF MS, FTIR, and UV–vis spectroscopy (Tables 1–5).

Table 6
Comparison of the EPR parameters of different radical adducts of various EMPO amino derivatives

Radical	HFS (G)	EMPO*		CAMPO		CAEPO		CAPPO		CABPO		CAPtPO	
		*trans***	*cis***										
·OOH		(94%)[x]	(6%)	(50%)	(50%)	(53%)	(47%)	(50%)	(50%)	(50%)	(50%)	(50%)	(50%)
	a_N	13.27 13.25	13.25	13.19	13.19	13.18	13.18	13.25	13.25	13.15	13.15	13.23	13.23
	a_N	12.37 9.30	10.15	9.89	12.09	9.95	12.25	9.50	11.90	9.71	12.01	9.80	12.00
	a_H	(55.5%/44.5% of *trans*[x])	1.50										
				(80%)[5]	(20%)[5]								
				a_N 13.0	13.1								
				a_H 10.8	12.5								
				a_H –	1.75								
		*trans***	*cis***										
·OH		(76%)	(24%)	(81%)	(19%)	(68%)	(32%)	(67%)	(33%)	(50%)	(50%)	(74%)	(26%)
	a_N	14.11	14.18	13.97	13.95	14.00	13.80	14.06	13.80	13.52	14.70	14.00	13.63
	a_H	12.80	15.27	13.64	12.45	14.85	11.65	14.71	11.67	13.75	22.00	14.95	12.05
	a_H	0.63	0.62	–	–	–	–	–	–	–	–	–	–
	a_H	0.43	0.50	(69%)[5]	(31%)[5]								
	a_H	0.21[(3)]	0.29[(3)]	a_N 14.0	14.0								
	a_H	0.13[(2)]	0.07[(2)]	a_H 13.5	12.5								
·H	a_N	(100%)		(100%)		(100%)		(100%)		(100%)		(100%)	
	a_N	15.52		15.30		15.16		15.21		15.17		15.20	
	a_H	22.21		22.23		23.12		23.05		23.09		23.03	
	a_H	20.82		20.00		19.35		19.37		19.39		19.39	
·CH_3		(100%)		(100%)		(54%)	(46%)	(53%)	(47%)	(53%)	(47%)	(50%)	(50%)
	a_N	15.42		15.15		15.06	15.06	15.06	15.06	15.06	15.06	14.97	14.47
	a_H	22.30		21.43		23.63	20.43	23.53	20.53	23.51	20.51	21.71	22.21
	a_H	–	–	–		–	–	–	–	–	–	–	–
·OCH_3		(50%)	(50%)	(74%)	(26%)	(100%)		(100%)		(100%)		(100%)	
	a_N	13.74	13.74	14.37	14.63	13.45		13.50		13.52		13.50	
	a_H	10.87	7.81	19.14	19.81	9.90		9.69		9.64		10.25	
	a_H	–	–	2.13	–	–		–		–			–
·CH_2OH		(100%)		(100%)		(63%)	(37%)	(63%)	(37%)	(69%)	(31%)	(60%)	(40%)
	a_N	14.95		14.75		14.50	14.70	14.53	14.70	14.53	14.72	14.54	14.74
	a_H	21.25		21.20		23.00	21.30	23.08	20.82	23.04	20.63	23.11	20.69
	a_H	–		–		–	1.45	–	1.20	–	1.20	–	1.20
·OC_2H_5		(50%)	(50%)	(74%)	(26%)	(100%)		(100%)		(100%)		(100%)	
	a_N	13.75	13.75	14.35	14.63	13.70		13.60		13.64		13.55	
	a_H	10.88	8.08	19.10	19.88	10.70		10.00		10.00		10.50	
	a_H	–	–	2.13	–	–		–		–		–	
·$CH(OH)CH_3$		(67%)	(33%)	(100%)		(50%)	(50%)	(50%)	(50%)	(50%)	(50%)	(50%)	(50%)
	a_N	14.94	15.00	14.77		14.90	14.30	14.85	14.35	14.85	14.35	14.95	14.45
	a_H	20.82	22.40	21.34		21.96	22.56	22.01	22.51	21.93	22.43	21.75	22.25
·CO_2^-		(100%)		(58/53[5]%)	(42/47[5]%)	(100%)		(100%)		(100%)		(100%)	
	a_N	14.74		14.46/14.53[5]	14.20/14.25[5]	14.04		14.06		14.07		14.05	
	a_H	17.16		16.62/16.48[5]	18.30/18.15[5]	19.31		19.15		19.15		19.24	
				[5]Villamena et al.									
NH_2 adduct (sec. product)		–		(100%)		(56%)	(44%)	(100%)		(53%)	(47%)	(54%)	(46%)
	a_N	–		14.43		14.38	14.10	14.30		14.30	14.05	14.30	14.05
	a_H	–		19.34		19.93	16.60	19.78		19.75	16.30	19.60	16.50
	a_N	–		2.17		2.18	2.85	2.15		2.40	2.70	2.40	2.70

*Data from Stolze et al.[12]; **data from Culcasi et al.[4] ([x]mixture of rotamers); [5]data from Villamena et al.[5].

Recent findings have shown that secondary products formed from decaying superoxide adducts can also be used as indicators of superoxide formation, especially when the relative ratios of diastereomers formed (*cis* and *trans* forms as well as rotamers) are considered.[14–18]

In order to draw unequivocal conclusions, however, well resolved ESR lines are a prerequisite, as well as the absence of secondary products formed in other side reactions.

We did not determine the rate constants of the superoxide trapping reactions, especially because of excessive formation of 5-amino adducts observed with all spin traps. Since the formation of the amino adducts was still observed after additional purification steps, we assume that the amino group is introduced by oxidative degradation of the 5-carbamoyl group to a 5-amino group (Hofmann degradation) and does not stem from impurities due to hydrolytic degradation of the amide group. Although the detection of the amino adduct was superoxide-dependent in the xanthine oxidase system (no adduct formed in the presence of SOD), it cannot be regarded as specific for superoxide, since it was also detected as a secondary product in other oxidizing systems, such as mixtures containing the spin trap and hypochlorite or incubations containing azide, hydrogen peroxide, and HRP (experiment not shown).

The stability of the hydroxyl radical adducts varied considerably. While the hydroxyl adducts of CAMPO (AMPO), CAEPO, and CAPPO were stable for 30 min or more, the respective adducts of CABPO and CAPtPO were stable only for a couple of minutes, forming as yet unknown secondary products, possibly due to attack at the alkyl side chain, followed by trapping by a second molecule of the spin trap, leading to broad, unresolved ESR lines. The relative change of the ratio between the different diastereomers does not seem to depend solely on the effect of steric hindrance of the 5-al-

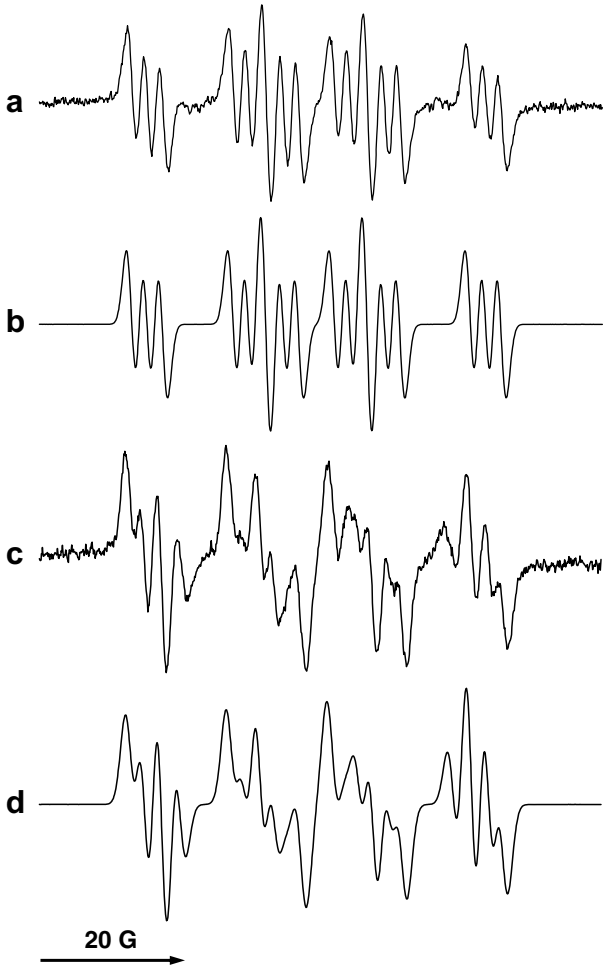

Figure 4. Amino adducts formed as secondary products from the hydroperoxide adducts of the spin traps CAMPO (AMPO) and CABPO. (a) CAMPO (AMPO) (20 mM), catalase (250 U/mL), xanthine (0.2 mM), and xanthine oxidase (500 mU/mL) in oxygenated phosphate buffer (20 mM, pH 7.4, containing 0.4 mM DTPA) were incubated for 10 min and measured using the following EPR parameters: sweep width, 80 G; modulation amplitude, 0.5 G; microwave power, 20 mW; time constant, 0.08 s; receiver gain, 5×10^4; and scan rate, 57 G/min. The spectrum shown is the secondary CAMPO (AMPO)/·NH_2 adduct seen after the decay of the initially formed CAMPO (AMPO)/·OOH adduct; (b) simulation of the EPR spectrum shown in Figure 2a. (c) Same as in (a), except that CABPO (20 mM) was used; and (d) Simulation of the EPR spectrum shown in Figure 2c.

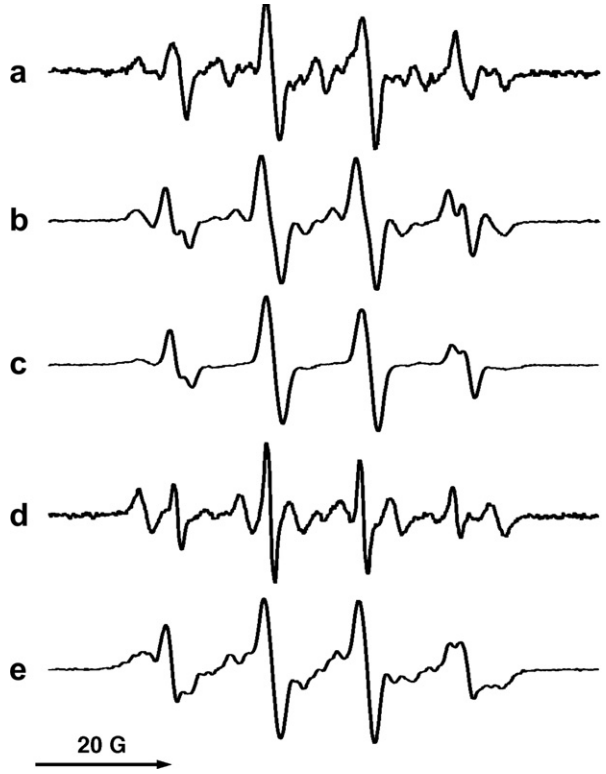

Figure 5. Formation of hydroxyl radical adducts of the spin traps CAMPO (AMPO), CAEPO, CAPPO, CABPO, and CAPtPO (a) CAMPO (AMPO) (40 mM, initial concentration) was incubated with a Fenton system containing $FeSO_4$ (1 mM), EDTA (2 mM), and H_2O_2 (0.2%). The reaction was stopped after 10 s by 1:1 dilution with phosphate buffer (300 mM, pH 7.4, containing 20 mM DTPA) and the spectrum was recorded using the following spectrometer settings: sweep width, 80 G; modulation amplitude, 0.21 G; microwave power, 20 mW; time constant, 0.08 s; receiver gain, 2×10^4; and scan rate, 57 G/min; (b) incubation as in (a), except that CAEPO (40 mM, init. conc.) was used; (c) incubation as in (a), except that CAPPO (40 mM, init. conc.) was used; (b) incubation as in (a), except that CABPO (40 mM, init. conc.) was used; and (b) incubation as in (a), except that CAPtPO (40 mM, init. conc.) was used.

kyl chain, since there is no gradual change from the ratio from the methyl to the pentyl derivatives, as can be seen in Table 6. Instead, a combination of steric and electronic factors seems to be responsible for the different stabilities of the diastereomers.

Methoxyl and ethoxyl radical adducts were rather unstable and difficult to detect, whereas carbon-centered adducts from methanol, ethanol, or formate were readily detectable.

4. Conclusion

In conclusion, the four novel EMPO-derived carbamoyl derivatives are forming superoxide adducts which were slightly more stable compared to the parent compound EMPO,[11,12,19–22] the most stable adduct (CAEPO/·OOH) being comparable to DEPMPO.[23] In addition, secondary products (amino adducts) are formed under oxidizing conditions which interfere with the EPR spectra of the initially formed adducts. In the case of CAMPO (AMPO), the intensity of the amino compound (SOD-sensitive) is very high for more than 30 min, so that further studies might be useful in order to elucidate their different pathways of formation (as those observed with azide/HRP).

5. Experimental

5.1. Chemicals

Acrolein and triethylamine were commercially available from Fluka, all other chemicals from VWR.

5.2. Syntheses

Synthesis and characterization of the compounds were performed in analogy to those reported previously[1–3] for the synthesis of EMPO and its derivatives[11,12,19–22] with minor adaptations as given below.

5.2.1. Synthesis of the ethyl 2-nitroalkanoates

The respective ethyl 2-bromoalkanoate (-propionate for CAMPO, -butanoate for CAEPO, -pentanoate for CAPPO, -hexanoate for CABPO, or -heptanoate for CAPtPO) was added under stirring to a solution of sodium nitrite (7.2 g, 104 mmol) and phloroglucinol (6.6 g, 52 mmol) in dry *N*,*N*-dimethyl formamide (120 ml) at room temperature. The solution was stirred overnight, poured into ice water (240 ml), and extracted four times with ethyl acetate

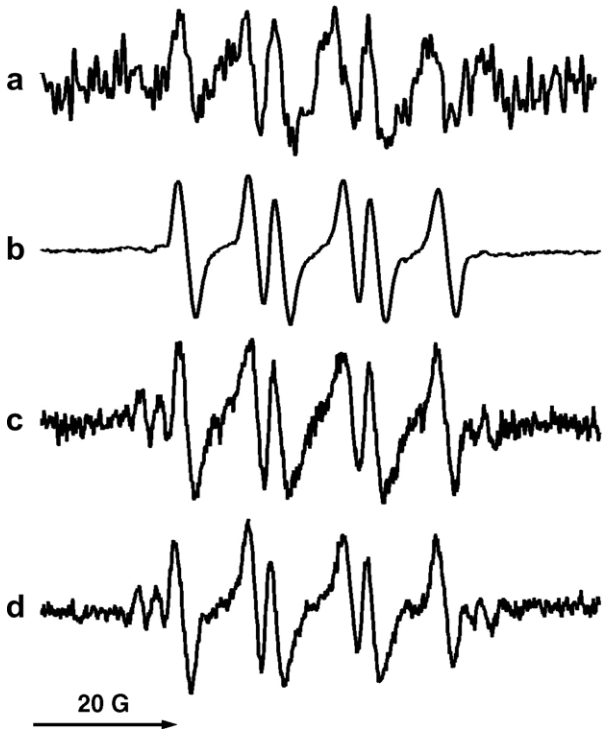

Figure 6. Formation of alkoxyl spin adducts from CAPPO and CAPtPO in the presence of methanol or ethanol. (a) After a 10 s incubation of CAPPO (1 M, init. conc. in methanol) with $FeCl_3$ (2 mM in methanol), the reaction was stopped by 1:20 dilution with phosphate buffer (0.3 M, pH 7.4, containing 20 mM DTPA), and the spectrum was recorded with the following spectrometer settings: sweep width, 80 G; modulation amplitude, 1.48 G; microwave power, 20 mW; time constant, 0.02 s; receiver gain, 2×10^5; and scan rate, 229 G/min; (b) same as in (a), except that CAPPO (1 M, init. conc. in ethanol) was used; (c) same as in (a), except that CAPtPO (1 M, init. conc. in methanol) was used; and (d) same as in (a), except that CAPtPO (1 M, init. conc. in ethanol) was used.

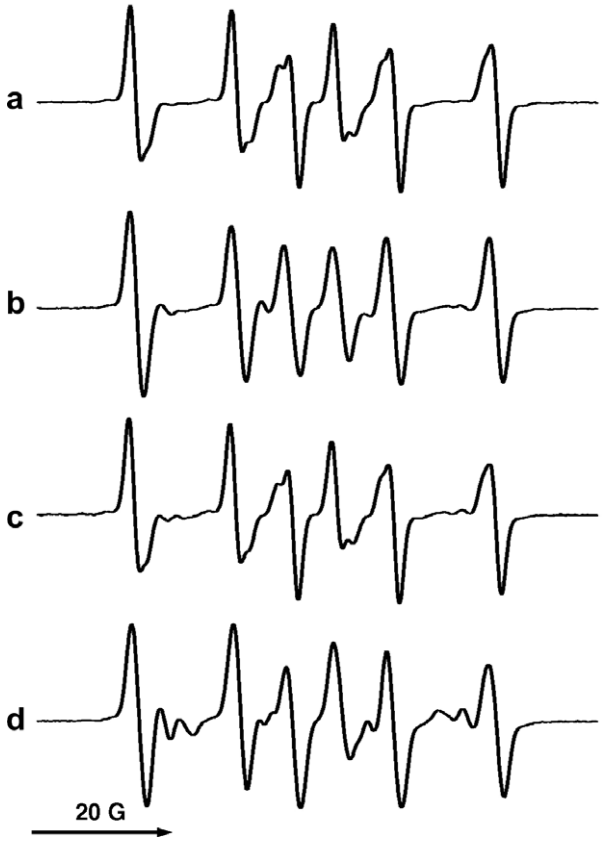

Figure 7. Iron-dependent formation of carbon-centered spin adducts from CAPPO and CAPtPO in the presence of methanol or ethanol. (a) CAPPO (40 mM, initial concentration) was incubated with a Fenton system containing $FeSO_4$ (1 mM), EDTA (2 mM), H_2O_2 (0.2%) in 10% methanol. The reaction was stopped after 10 s by 1:1 dilution with phosphate buffer (300 mM, pH 7.4, containing 20 mM DTPA) and the spectrum was recorded using the following spectrometer settings: sweep width, 80 G; modulation amplitude, 0.21 G; microwave power, 20 mW; time constant, 0.08 s; receiver gain, 4×10^4; scan rate, 57 G/min; (b) same as in (a), except that ethanol was used; (c) same as in (a), except that CAPtPO was used; and (d) same as in (a), except that CAPtPO and ethanol were used.

(100 ml). The combined extracts were treated with 100 ml of a $NaHCO_3/Na_2CO_3$ solution and dried over $MgSO_4$. After removal of the solids by filtration, the solvent was evaporated in vacuo. Deeply colored products were extracted with water. After removal of the solvent from the organic phase, the pale yellow product was used without further purification the aqueous phase (containing the major part of the colored impurities) was discarded. Average yield: 85% (crude product).

5.2.2. Ethyl 2-alkyl-2-nitro-4-oxobutanoate

The respective ethyl 2-nitroalkanoate was dissolved in a mixture of acetonitrile (10 g, 244 mmol) and triethylamine (0.2 g, 2 mmol). Acrolein (2 g, 38 mmol) was slowly added at 0 °C. The solution was kept at 10 °C for 1.5 h and then poured into a solution of ice-cold HCl (5 ml of concentrated HCl in 150 ml of water). The solution was extracted three times with CH_2Cl_2 and dried over $MgSO_4$. After filtration, the mixture was distilled under reduced pressure, and the purity of the remaining product was assessed by thin layer chromatography and IR spectroscopy. Average yield: 84% (crude product).

5.2.3. Synthesis of the nitrones

Synthesis of the nitrones was performed according to the procedure described recently for the synthesis of EMPO derivatives.[1–3,11,12] To a concentrated solution of 25 mmol of the respective ethyl-2-alkyl-2-nitro-4-oxobutanoate in H_2O/CH_3OH (v/v = 6:4), an aqueous solution of ammonium chloride (1.87 g in 8 ml of water) was added. While zinc dust (8.5 g, 130 mmol) was slowly added within 30 min, the mixture was carefully kept at room temperature. The mixture was stirred for 4.5 h at room temperature, the white precipitate and the remaining zinc powder were removed by filtration, and the residue was washed five times with methanol (30 ml). The liquid phase was concentrated to about 10 ml and extracted four times with 60 ml CH_2Cl_2. The organic phase was dried with $MgSO_4$, filtered, and concentrated. Column chromatography on silica gel with a petroleum ether/ethanol gradient allowed the separation from the majority of side products and provided a dark yellow or light brown product. Additional purification was done on a 1 ml solid phase extraction column using a Chromabond C-18 100 mg column obtained from Macherey-Nagel (Düren, Germany), using a water/methanol gradient as the eluant. Colored solutions were subjected to the same procedure until the solution containing the *N*-oxides remained colorless. The products were extracted three times with CH_2Cl_2, the solvent was removed, and the identity checked by TLC, IR, and UV–vis spectroscopy. Average yield: 46% (purified product).

5.2.4. Synthesis of the 5-alkyl-5-carbamoylpyrroline *N*-oxides

Synthesis of the 5-alkyl-5-carbamoylpyrroline *N*-oxides was performed according to Villamena et al.[5,6] Briefly, the respective nitrones (EMPO, EEPO, EPPO, EBPO, and EPtPO) were dissolved in aqueous ammonia solution and stirred for several days until the spot (TLC) or peak (HPLC) of the original *N*-oxide had completely

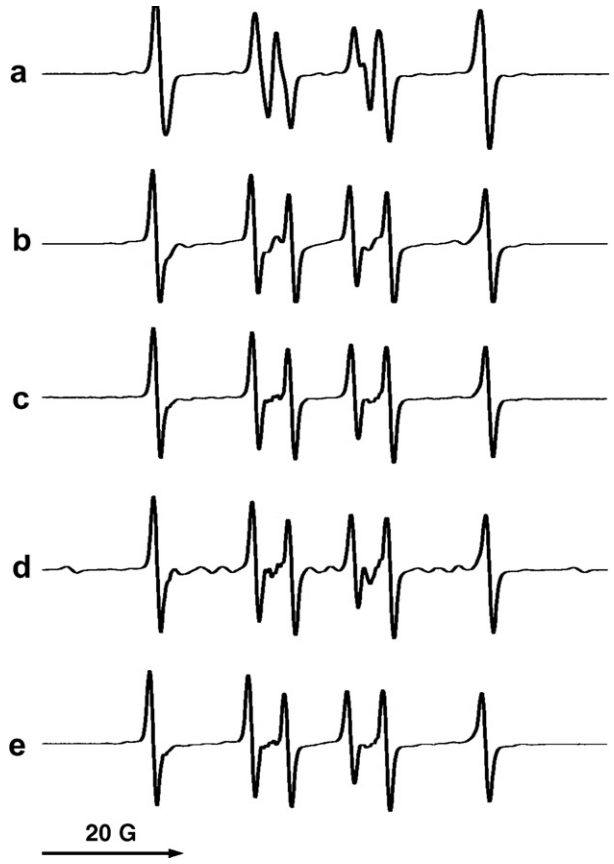

Figure 8. Iron-dependent formation of carbon-centered spin adducts from CAMPO, CAEPO, CAPPO, CABPO, and CAPtPO in the presence of formate. (a) CAMPO (40 mM, init. conc.) was incubated with a Fenton system containing $FeSO_4$ (1 mM), EDTA (2 mM), H_2O_2 (0.2%), and sodium formate (200 mM). The reaction was stopped after 10 s by 1:1 dilution with phosphate buffer (300 mM, pH 7.4, containing 20 mM DTPA), and the spectrum was recorded using the following spectrometer settings: sweep width, 80 G; modulation amplitude, 0.2 G; microwave power, 20 mW; time constant, 0.08 s; receiver gain, 5×10^4; scan rate, 57 G/min; (b) same as in (a), except that CAEPO was used; (c) same as in (a), except that CAPPO was used; (d) same as in (a), except that CABPO was used; and (e) same as in (a), except that CAPtPO was used.

disappeared. If dark colored secondary products were formed in larger amounts (e.g., during the synthesis of CAMPO), the incubation was stopped earlier. After removal of the aqueous ammonia solution, the crude products were subjected to column chromatography on silica gel using methylene chloride/ethanol mixtures as the eluants. After purification on 1 ml solid phase extraction columns as described above (Chromabond C-18 100 mg columns), the compounds were obtained as white crystals or colorless oils that crystallized in the refrigerator after several days. The purity of the obtained products was assessed by TLC and UV–vis spectroscopy. Final identification of the purified products was performed by ^{1}H NMR, ^{13}C NMR, and IR spectroscopy. Purity was confirmed by HRMS (see Tables 1–4). Average yield: 29% (purified product).

5.3. Instruments

NMR spectra were recorded on a Bruker Avance at 400 MHz for ^{1}H, and 100 MHz for ^{13}C at 22 °C. $CDCl_3$ was used as the solvent throughout, TMS (tetramethylsilane) as the internal standard. Concentrations were set to 10 mg sample/0.6 ml solvent. ^{13}C peaks were assigned by means of APT (attached proton test), HMQC (^{1}H-detected heteronuclear multiple-quantum coherence), and HMBC (heteronuclear multiple bond connectivity) spectra. All chemical shift data are given in ppm units (Tables 1 and 2).

Mass spectra were obtained as follows (Table 3): Samples were diluted in the ratio 1:10,000 in 70% methanol containing 0.1% formic acid and injected offline to ESI Q-TOF MS on a Waters Micromass Q-TOF Ultima Global at a flow rate of 5 μl/min. Capillary voltage was adjusted bewteen 1.2 and 3.0 kV. Data analysis was performed with MassLynx 4.0 SP4 Software (Waters Micromass).

IR spectra were recorded as film on an ATI Mattson Genesis Series FTIR spectrometer (see also Table 4).

UV–vis spectra were recorded on Hitachi 150-20 and U-3300 spectrophotometers in double-beam mode against a blank of the respective solvent (Table 5). Determination of the concentrations was done measuring the absorption maxima in the range between 200 and 300 nm. For determination of the partition coefficients, 500 μl of *n*-octanol was added to 500 μl of a solution of the respective spin trap (100 mM or 5–10 mg, respectively) in 100 mM phosphate buffer, pH 7.4. The mixture was vortexed for 2 min at room temperature. If necessary, the procedure was repeated several times, until equilibration between the two phases was achieved. After careful separation of the phases, the absorbance was read at the maximum around 235 nm after dilution with methanol. For EPR experiments, Bruker spectrometers (ESP300E and EMX) were used, operating at 9.7 GHz with 100 kHz modulation frequency, equipped with a rectangular TE_{102} or a TM_{110} microwave cavity. All calculations for spectral simulation were done using the SinFonia Program by Bruker (Table 6).

Acknowledgments

The authors thank P. Jodl for skilful technical assistance in synthesis, purification, and characterization of the spin traps.

References and notes

1. Stolze, K.; Rohr-Udilova, N.; Rosenau, T.; Stadtmüller, R.; Nohl, H. *Biochem. Pharmacol.* **2005**, *69*, 1351.
2. Stolze, K.; Rohr-Udilova, N.; Rosenau, T.; Hofinger, A.; Kolarich, D.; Nohl, H. *Bioorg. Med. Chem.* **2006**, *14*, 3368.
3. Stolze, K.; Rohr-Udilova, N.; Rosenau, T.; Hofinger, A.; Nohl, H. *Bioorg. Med. Chem.* **2007**, *15*, 2827.
4. Culcasi, M.; Rockenbauer, A.; Mercier, A.; Clément, J.-L.; Pietri, S. *Free Radic. Biol. Med.* **2006**, *40*, 1524.
5. Villamena, F. A.; Rockenbauer, A.; Gallucci, J.; Velayutham, M.; Hadad, C. M.; Zweier, J. L. *J. Org. Chem.* **2004**, *69*, 7994.
6. Villamena, F. A.; Xia, S.; Merle, J. K.; Lauricella, R.; Tuccio, B.; Hadad, C. M.; Zweier, J. L. *J. Am. Chem. Soc.* **2007**, *129*, 8177.
7. Gamliel, A.; Afri, M.; Frimer, A. A. *Free Radic. Biol. Med.* **2008**, *44*, 1394.
8. Chignell, C. F.; Kalyanaraman, B.; Sik, R. H.; Mason, R. P. *Photochem. Photobiol.* **1981**, *34*, 147.
9. Kirino, Y.; Ohkuma, T.; Kwan, T. *Chem. Pharm. Bull.* **1981**, *29*, 29.
10. Dikalov, S. I.; Mason, R. P. *Free Radic. Biol. Med.* **2001**, *30*, 187.
11. Stolze, K.; Udilova, N.; Nohl, H. *Biol. Chem.* **2002**, *383*, 813.
12. Stolze, K.; Udilova, N.; Rosenau, T.; Hofinger, A.; Nohl, H. *Biol. Chem.* **2003**, *384*, 493.
13. Roubaud, V.; Lauricella, R.; Bouteiller, J. C.; Tuccio, B. *Arch. Biochem. Biophys.* **2002**, *397*, 51.
14. Tsai, P.; Marra, J. M.; Pou, S.; Bowman, M. K.; Rosen, G. M. *J. Org. Chem.* **2005**, *70*, 7093.
15. Villamena, F. A.; Hadad, C. M.; Zweier, J. L. *J. Am. Chem. Soc.* **2004**, *126*, 1816.
16. Karoui, H.; Clément, J.-L.; Rockenbauer, A.; Siri, D.; Tordo, P. *Tetrahedron Lett.* **2004**, *45*, 149.
17. Rockenbauer, A.; Clément, J.-L.; Culcasi, M.; Mercier, A.; Tordo, P.; Pietri, S. *J. Phys. Chem A* **2007**, *111*, 4950.
18. Clément, J.-L.; Ferré, N.; Siri, D.; Karoui, H.; Rockenbauer, A.; Tordo, P. *J. Org. Chem.* **2005**, *70*, 1198.
19. Olive, G.; Mercier, A.; LeMoigne, F.; Rockenbauer, A.; Tordo, P. *Free Radic. Biol. Med.* **2000**, *28*, 403.
20. Zhang, H.; Joseph, J.; Vasquez-Vivar, J.; Karoui, H.; Nsanzumuhire, C.; Martásek, P.; Tordo, P.; Kalyanaraman, B. *FEBS Lett.* **2000**, *473*, 58.
21. Zhao, H.; Joseph, J.; Zhang, H.; Karoui, H.; Kalyanaraman, B. *Free Radic. Biol. Med.* **2001**, *31*, 599.
22. Weaver, J.; Tsai, P.; Pou, S.; Rosen, G. M. *J. Org. Chem.* **2004**, *69*, 8423.
23. Fréjaville, C.; Karoui, H.; Tuccio, B.; Le Moigne, F.; Culcasi, M.; Pietri, S.; Lauricella, R.; Tordo, P. *J. Med. Chem.* **1995**, *38*, 258.